Sound induces change in orientation preference of V1 neurons: Audio-visual cross-influence

Nayan Chanauria[1], Vishal Bharmauria[2], Lyes Bachatene[3], Sarah Cattan[4], Jean Rouat[5], Stéphane Molotchnikoff[1]

[1]Neurophysiology of Visual System, Département de Sciences Biologiques, Université de Montréal, CP 6128 Succursale Centre-Ville, Montréal, QC H3C 3J7, Canada

[2]The Visuomotor Neuroscience Lab, Centre for Vision Research, Faculty of Health, York University, Toronto, ON, Canada

[3]Department of Nuclear Medicine and Radiobiology, Faculty of Medicine and Health Sciences (CHUS), SNAIL, Sherbrooke Neuro Analysis and Imaging Lab, University of Sherbrooke, Sherbrooke, QC, Canada

[4]Institut de Neuroscience de la Timone, Faculté de Médecine, 27, Boulevard Jean Moulin 13005 Marseille, France

[5]Departement de Génie Électrique et Génie Informatique, Université de Sherbrooke, Sherbrooke, QC, Canada

Abstract

In the cortex, demarcated unimodal sensory regions often respond to unforeseen sensory stimuli and exhibit plasticity. The goal of the current investigation was to test evoked responses of the primary visual cortex (V1) neurons when an adapting auditory stimulus was applied in isolation. Using extracellular recordings in anesthetized cats, we demonstrate that, unlike the prevailing observation of only slight modulations in the firing rates of the neurons, sound imposition in isolation entirely shifted the peaks of orientation tuning curves of neurons in both supra- and infra-granular layers of the V1. Our results suggest that neurons specific to either layer dynamically integrate features of the sound and modify the organization of orientation map of V1. Intriguingly, these experiments present novel findings that the mere presentation of a prolonged auditory stimulus may drastically recalibrate the tuning properties of the visual neurons and highlight the phenomenal neuroplasticity of V1 neurons.

Introduction

Although, inputs to a primary sensory area have been thought to be largely modality specific, an emerging notion proposes a direct and more specific interaction between the early sensory cortices of different modalities (Kayser & Logothetis, 2007). Per se, regions like the primary visual cortex (V1) are conservative and considered to be excited exclusively by visual input. Multimodal research has steered a new insight into the brain organization and perception. Several studies have suggested that the meeting and interaction of information from different senses begin within the low-level sensory areas (Ghazanfar & Schroeder, 2006; van Atteveldt *et al.*, 2014; Ten Oever *et al.*, 2015). Further, more findings propose that even low-order sensory areas may contribute to multisensory processing starting from a very early stage (Schroeder *et al.*, 2003; Foxe & Schroeder, 2005; Macaluso & Driver, 2005). fMRI studies also support this line of thought (Clavagnier *et al.*, 2004; Kayser *et al.*, 2005). Studies in non-human primates have revealed direct cortico-cortical pathways from the primary auditory (A1) to the primary visual cortex (V1) (Rockland & Van Hoesen, 1994; Falchier *et al.*, 2002; Rockland & Ojima, 2003; Clavagnier *et al.*, 2004; Budinger *et al.*, 2006). Direct anatomical connections from V1 to A1 are not precisely known, but it has been shown that secondary visual area V2 is directly connected with A1 (Budinger *et al.*, 2006). An alternative yet slightly longer pathway between A1 and V1 through the heteromodal association cortical area (superior temporal polysensory area and superior temporal sulcus (STP / STS))was also thought to send feedback to both A1 and V1 (Schroeder & Foxe, 2002). A critical study (Liang *et al.*, 2013) revealed that there might be salient locations within V1 that respond to specific cross-modal inputs related to the spatial pattern of activation of a primary sensory cortical area (e.g., V1). On similar lines, Lomber and colleagues have demonstrated in congenitally and early deaf cats that the auditory cortex including associated areas undergo crucial cross-modal interactions wherein visual cortex displays the functions of the auditory cortex, especially in the absence of acoustic input (Kral & Lomber, 2015; Land *et al.*, 2016; Meredith *et al.*, 2016; Butler *et al.*, 2017; Clemo *et al.*, 2017). Furthermore, it has been shown in humans that reaction-time speeds up when sensory information from different modalities is combined

(Hershenson, 1962; Gielen *et al.*, 1983). A similar study from McDonald and colleagues(McDonald *et al.*, 2013) demonstrated that sound automatically activates visual cortex in a spatial specific manner. Two recent cases enabled to understand different facets of cross-modal processing in V1. Ibrahim and co-authors (Ibrahim *et al.*, 2016) demonstrated sharpening of orientation tuning in conjunction with an enhancement of the response to the preferred orientation of the cell, predominantly when a low-contrast visual stimulus was accompanying an auditory stimulus. On the contrary, Iurilli and colleagues (Iurilli *et al.*, 2012) revealed that presentation of a high-amplitude sound stimulus resulted in the hyperpolarization of the membrane potential of V1 neurons resulting in inhibition. From above findings, it appears that sensory regions of the cortex particularly V1 neurons adopt a different outline of processing towards the multimodal configuration of stimulus features.

Despite extensive experimentation to explore multimodal interactions in the cortex, the role of cross-modal inputs in modulating sensory processing features of cortical neurons and the precise underlying mechanisms remain unstated. To date, most studies have limited the presentation of stimuli for a very short duration. Additionally, mostly rodents have been the first choice for electrophysiological experimentation in this direction and imaging is being fully exploited in humans. In the present investigation, a sound stimulus was applied to V1 neurons in cats in the complete absence of a visual input for 12 minutes. To this goal, through extracellular recordings in area 17 of anesthetized cats, we found that in the presence of a non-visual input, in our case a sound stimulus, the orientation tunings of simultaneously recorded layer 2/3 and layer 5/6 visual neurons were fully altered while exhibiting shifts in their tuning. Also, the orientation shift magnitude was found to be larger in layer 5/6 neurons. We argue and suggest that the modification was solely potentiated by the continuous repetition of the sound stimulus for 12 min and the spatial-temporal structure of the sound. Interestingly, layer 2/3 neurons displayed an intriguing shift pattern towards horizontal orientations unlike cells of layer 5/6. Our data illustrate a novel extension to audio-visual cross-influence demonstrating that even an isolated application of a sound can robustly induce a reorganization of area V1. Our data exemplifies supramodal nature and cross-modal

interactions in the V1 that possibly occur early during a multisensory integration process in response to a sensory stimulus that differs in its expected matching response region.

Materials and methods

Ethical approval

Eight adult domestic cats (*Felis catus*) of either sex were used for experiments adhering to the guidelines approved by the NIH in the USA and the Canadian Council on Animal Care. Cats were supplied by the Division of Animal Resources of the University of Montreal. The animal surgery and electrophysiological recording procedures were performed according to the guidelines of the Canadian Council on Animal Care and were approved by the Institutional Animal Care and Use Committee of the University of Montreal (CDEA).

Anesthesia

Cats were initially sedated with a mixture of Atravet (0.1 mg/kg, s.c.,Wyeth-Ayerst, Guelph, ON, Canada) and atropine sulphate (0.04 mg/kg, s.c., Atrosa; Rafter, Calgary, AB, Canada) followed by a dose of anesthetic ketamine (40 mg/kg, i.m., Narketan; Vetoquinol, QC, Canada). Anesthesia was maintained during the surgery with isoflurane ventilation (2%, AErrane; Baxter, Toronto, ON, Canada). After the surgery, cats were fixed on the stereotaxic and were paralyzed by perfusion of gallamine triethiodide (40 mg/kg, i.v., Flaxedil; Sigma Chemical, St Louis, MO, USA). Artificial ventilation was maintained by a mixture of O2/N2O (30: 70) and isoflurane (0.5%). The paralysis was continued by perfusion of gallamine triethiodide (10 mg/kg/h) in 5% dextrose lactated Ringer’s nutritive solution (i.v., Baxter, Mississauga, ON, Canada) throughout the experiment.

Surgery

Local anesthetic xylocaine (2%; AstraZeneca, Mississauga, ON, Canada) was injected subcutaneously during the surgery before any opening of the skin. A heated pad was placed beneath the cat to maintain a body temperature of 37.5 °C. Antibiotics Tribrissen (30 mg/kg/day, subcutaneous; Schering Plough, Pointe-Claire, QC, Canada) and Duplocillin (0.1 mL/kg, intra-muscular; Intervet, Withby, ON, Canada) were administered to the animals to prevent bacterial infection. First, a vein of the animal's forelimb was cannulated. Then tracheotomy was performed to artificially ventilate the animal. A proper depth of anesthesia was ensured throughout the experiment by monitoring the EEG, the electrocardiogram, and the expired CO2. O2 saturation was kept in check using an Oximeter. The end-tidal CO2 partial pressure was kept constant between 25 and 30 mmHg. Third, craniotomy (1*1 cm) was performed over the primary visual cortex (area 17/18, Horsley-Clarke coordinates P0-P6; L0-L6). The underlying dura was removed, and the depth electrode was positioned in area 17. The pupils were dilated with atropine sulfate (1%; Isopto-Atropine, Alcon, Mississauga, ON, Canada) and the nictitating membranes were retracted with phenylephrine hydrochloride (2.5%; Mydfrin, Alcon). Plano contact lenses with artificial pupils (5 mm diameter) were placed on the cat's eyes to prevent the cornea from drying. Finally, the cats were sacrificed with a lethal dose of pentobarbital sodium (100 mg/kg; Somnotol, MTC Pharmaceuticals, Cambridge, ON, Canada) by an intravenous injection.

Stimuli and experimental design

Two types of stimuli were used in the experiments- visual and audio. First, the receptive fields were located centrally within a 15° radius from the fovea. Monocular stimulation was performed. Receptive field edges (RF) were explored once clear detectable activity was obtained using a handheld ophthalmoscope (Barlow *et al.*, 1967). This was done by moving a light bar from the periphery toward the center until a response was evoked. Contrast and mean luminance was set at 80% and 40cd/m^2, respectively. Optimal spatial and temporal frequencies were set at 0.24 cycles/deg and in the range 1.0–2.0 Hz (at these values V1 neurons are driven maximally) for drifting sine-wave gratings (Bardy *et al.*, 2006). Then, gratings were presented randomly as visual stimuli covering the excitatory RF to compute the

orientation tuning curves of neurons (Maffei *et al.*, 1973). Visual stimuli were generated with a VSG 2/5 graphics board (Cambridge Research Systems, Rochester, England) and displayed on a 21-inch Monitor (Sony GDM-F520 Trinitron, Tokyo, Japan) placed 57 cm from the cat's eyes, with 1024×9×768 pixels, running at 100 Hz frame refresh (Figure 1 A). The gratings moved unidirectionally in eight possible orientations presented randomly one by one. Each randomly presented oriented grating was given 25 times for 4s each with an inter-stimulus interval of 1-3s. Subsequently, the animal was exposed to broadband noise-like auditory stimuli comprising a range of frequencies. The auditory stimulus (3s 78 dB SPL) consisted of temporally orthogonal rippled combinations (TORC's) with varying frequency components from 250 Hz to 8000 Hz (Fries *et al.*, 2007). The 3s stimulus was played continuously for 12 minutes, was delivered by a pair of external loudspeakers (120 Hz-18 KHz) and positioned perpendicularly relative to the animal axis at 57 cm to the center of the fixation axis of the animal. For some recordings, the speakers were also displaced laterally at the same plane, at 30 cm on either side from the center of the fixation axis of the cat. This was done to test the difference in responses when the position of speakers was changed. The sound frequency and intensity were cyclical and optimized and set according to the experiment design using Bruel and Kjaer Spectris Group Sonometer. The stimulus was optimized on a standard C-scale of the sonometer for both ears. The spectrogram of the sound stimulus displaying varying frequencies is shown in Figure 1 B. After the 12-min presentation of the acoustic stimulus, a series of drifting gratings was presented again in a random order (each oriented grating presented 25 times, 4s each and inter-stimulus time interval). It must be emphasized that sound was applied in isolation, that is, no visual stimulus was presented during the sound application. Finally, a recovery period of 90 minutes was given for neurons to return to their optimal state (Figure 1 C).

Electrophysiology

Multiunit activity in the primary visual cortex of anesthetized cats was recorded using a tungsten multichannel depth electrode (0.1–0.8 MΩ at 1 KHz; Alpha Omega Co. USA Inc). Neural activity was recorded from both hemispheres of the cat's brain. The depth electrode consisted of four microelectrodes

enclosed in a stainless-steel tubing in a linear array with an inter-electrode spacing of 500 µm. The recorded signal from the microelectrodes was acquired using Spike2, CED, Cambridge, UK. The signal was further amplified, band-pass filtered (300 Hz–3 KHz), digitized, displayed on an oscilloscope and recorded with a 0.05 ms temporal resolution. Recordings were performed at average cortical depths of 300–500 µm and 1000–1200 µm (Chanauria *et al.*, 2016) simultaneously from both sites as depicted in Figure 1 D. Spike sorting was done offline using same Spike2 package, CED, Cambridge, UK. Figure 2 shows an example of neuronal isolation (spike sorting) from the multiunit activity. As a precautionary measure, it was essential to affirm that we did not isolate the same unit twice, as the same unit may exhibit different waveforms depending upon several factors. Thus, the single units were discriminated based upon the spike waveforms, principal component analysis (PCA), and autocorrelograms (ACG) (Bharmauria *et al.*, 2015; Bharmauria *et al.*, 2016). The respective PCA, ACGs, and spike waveforms are also shown along in Figure 2.

Data Analysis

Tuning curves

After sorting neurons offline, the numerical value of orientation selectivity was calculated for each neuron at control and post-sound presentation conditions. Since applied gratings were separated by intervals of 22°, orientation tuning curves values were obtained by fitting a Gaussian non-linear curve on the raw orientation tuning values obtained at each orientation for each neuron. The Gaussian tuning fits were computed using the function below:

$$\boldsymbol{y} = \boldsymbol{y0} + \left(\boldsymbol{A} \div \left(\boldsymbol{w} \times \sqrt{\left(\frac{\pi}{2}\right)}\right)\right) \times \boldsymbol{e}^{\left(-2\times\left(\frac{(X-XC)}{w}\right)^2\right)} \qquad \text{(Equation 1)}$$

where *y0* is the offset, *XC* is the center, *w* is the width, and *A* represents the area under the Gaussian fit. The firing rates were normalized and gaussian tuning curves were generated in the scientific software

Origin. The above procedure indicates the preferred orientation with better accuracy. The same method was carried in controls and following sound adaptation. The magnitude of shifts was computed as the distance (subtractions) between peak positions of the fitted Gaussian tuning curves before and after the presentation of sound (the difference between the initially preferred and newly acquired). The following formula was applied to calculate the shift magnitudes:

Shift magnitude = $(XC_{Post} - XC_{Pre})$ (Equation 2)

where XC is the central value derived from the Gaussian fit.

According to past studies, a difference of > 5º is considered as a significant shift (Ghisovan *et al.*, 2009; Bachatene *et al.*, 2012a; Bachatene *et al.*, 2013; Bachatene *et al.*, 2015; Chanauria *et al.*, 2016). A magnitude of <5º indicated a neuron that retained its initially preferred orientation even after the presentation of sound. These calculations are critical as the interval of 22° between the stimulus orientations is relatively large, which makes it difficult to deduce an exact value of orientation tuning from only raw curves.

Orientation Selectivity Index (OSI)

Further, the Orientation Selectivity Index (OSI) of each neuron was computed by dividing the firing rate of the neuron at the orthogonal orientation by the firing rate of the same neuron at the preferred orientation, and subtracting the result from 1 (Ramoa *et al.*, 2001; Liao *et al.*, 2004). The closer the OSI is to 1, the stronger the orientation selectivity.

Orientation Selectivity Index = $1 - (FR_{Orthogonal} / FR_{Preferred})$ (Equation 3)

where FR is the firing rate of the same neuron.

Bandwidths (BW)

Tuning bandwidths were calculated based on the full width at half magnitude (FWHM) of the Gaussian tuning curves for each neuron (Ringach *et al.*, 2002; Moore *et al.*, 2005). Bandwidths are measured to deduce the sharpness of orientation tuning curves of the neurons.

$$\text{FWHM (Bandwidth)} = 2\sqrt{2\ \ln 2}\ c \quad = 2.35482c \qquad \text{(Equation 4)}$$

where ln is the logarithm and c is the gaussian root mean square width.

Response Change Index (RCI)

To quantify the response disparity between stimulus conditions for each neuron, the traditional method of measuring response change index was used (Stevenson *et al.*, 2014; Meijer *et al.*, 2017) where the values of the RCI are normalized and can be used as a parameter to describe both enhancement and suppression. The values may range from -1 to 1 in which negative values indicate response suppression and positive values indicate response enhancement.

$$RCI = (FR_{Postsound} - FR_{Control}) / (FR_{Postsound} + FR_{Control}) \quad \text{(Equation 5)}$$

where FR is firing rate of the same neuron

Statistical tests

Five datasets from layer 2/3 and layer 5/6 were tested for statistics values of (i) orientation tunings of neurons (ii) amplitudes of shift; (iii) OSI of neurons at pre- and post-sound presentation conditions; and (iv) Bandwidth (v) Response Change Index. These data were tested for normal distribution using the Shapiro Wilk normality test. Based on the results obtained, parametric and non-parametric tests were applied on data sets. Consequently, comparisons were drawn between values of different parameters for either layer. Detailed information of tests can be found in legends of the figures as well as the results. The current investigation focused on how visual cells reacted towards oriented gratings when a sound stimulus

was presented solely in the absence of any other visual stimulation. The extracellular activity of V1 neurons was simultaneously recorded from the layer 2/3 and 5/6 down the column. The gaussian tuning curves of neurons in layer 2/3 and layer 5/6 were compared between the control and post-sound situations. In total, 239 cells were recorded during different experiments out of which 124 neurons belonged to the layer 2/3 and remaining 115 to the layer 5/6. These pools were used for further analysis and statistics.

Results

Impact of repetitive auditory input on orientation tuning of visual neurons: A typical example

Unlike previous studies where a modulation of response was remarked after the presentation of auditory stimulus for a few milliseconds (Iurilli *et al.*, 2012; Ibrahim *et al.*, 2016), intriguingly, in this investigation, a complete shift in the curves of the orientation tuning of neurons was observed following the sound application. Figure 3 shows the typical result of a recorded neuron pair from layer 2/3 and layer 5/6. Two typical orientation tuning curves in raw forms are shown as (A) and (C) for layer 2/3 and layer 5/6 respectively. To infer the exact value of orientation preference, non-linear Gaussian fits were generated and are shown for the supra-granular (Figure 3B) and infra-granular cell (Figure 3D) for either condition. It must be emphasized that both cells were recorded simultaneously from the same electrode and the recording sites were separated by ~500 microns. The supra-granular cell exhibited an optimal orientation at 94.29° deg while the optimal orientation of the infra-granular layer was 96.70° suggesting that the electrode was lowered in the same orientation column, since optimal orientations are about equal. Following sound application, both cells displayed a novel optimal orientation. The peak of the optimal orientation of the supra-granular cell shifted to 110.92° indicating a displacement of 16° whereas the peak of the infra-granular cell moved in the opposite direction to 74.94° demonstrating shift amplitude of 21°. The opposite displacement of the peaks of optimal orientation tuning suggests that these shifts cannot be attributed to a global and spontaneous fluctuation of the firing rates. Each cell behaved independently. Furthermore, numerous studies have shown that, while the magnitude of the optimal responses may vary,

the optimal orientation preference exhibits stability. Indeed, the optimal orientation remains same for hours and even days and these controls were shown by Bachatene and colleagues (Bachatene *et al.*, 2015) (Henry *et al.*, 1973; Frenkel *et al.*, 2006; Lutcke *et al.*, 2013). Therefore, the significant change in orientation selectivity is due to the experience of visual neurons with the sound.

Shift amplitude and sound source localization

The extent of shift amplitude of the orientation tuning curves is illustrated in Figure 4. The shift amplitudes were calculated by subtracting the numerical values of orientation selectivity obtained at control and post-sound conditions. On this dataset, a non-parametric statistical method was applied. The significant differences are indicated by solid black lines above each plot. The graphs A-C display values of orientation tuning when speakers were placed laterally on either side of the animal with respect to the fixation axis of the animal. The graph shows the difference in tuning curves pre- and post-sound for layer 2/3 neurons, which was found to be significantly different (Wilcoxon matched-pairs signed rank test, $P < 0.001$). In layer 2/3 (refer to Figure 4 A), the preferred orientations of the neurons appeared to have a significant bias towards horizontal orientations (range 0° to 50°) whereas this trend was not observed in layer 5/6 (refer to Figure 4 B) wherein the orientation preference shifts covered the full spread of presented gratings (range 0° to 157.5^0). The significant bias observed could be attributed to the properties of the stimulus itself or to the distinct mechanisms that drive the multimodal interaction between auditory and visual cortex. The over-all mean values for the three experimental steps (control, post sound application, recovery about one hour following sound application) are shown in histogram inserts, indicating a full recovery. Further, mean shifts of layer 2/3 and 5/6 neurons at control and post-sound conditions were compared using One-way ANOVA (refer to Figure 4 C). The means (mean ± SEM) for the four mentioned datasets were 81.41 ± 4.95, 18.15 ±1.88, 83.33 ± 4.56 and 71.38 ± 4.33 respectively. These four data sets were compared with one another using Tukey's multiple post comparison test. Three out of six groups, (layer 2/3 control versus layer 2/3 post-sound, layer 2/3 post-sound versus layer 5/6 control and layer 2/3 post-sound versus layer 5/6 post-sound), were found significantly different whereas

the remaining three groups (layer 2/3 control vs layer 5/6 control, layer 2/3 control vs layer 5/6 post-sound and layer 5/6 control versus layer 5/6 post-sound) were found statistically non-significant.

To explore the effects of displacement of the sound source, the speakers were positioned in the front of the animal. No critical statistical difference (Wilcoxon matched-pairs signed rank test, P-value = 0.8984) was observed in the orientation tuning values at both conditions for layer 2/3 neurons (N = 08, Figure 5A) and layer 5/6 neuron's (N = 11, Figure 5B). The mean amplitudes for layer 2/3 and layer 5/6 neurons at control and post-sound conditions were compared and found non-significant (One-way ANOVA). The means (mean ± SEM) for the mentioned four datasets were found to be 69.34 ± 13.21, 14.79 ± 4.90, 90.22 ± 11.91 and 91.24 ± 11.38 respectively (Figure 5 C). Using Tukey's multiple post comparison test three out of six groups, (layer 2/3 control vs layer 2/3 post-sound, layer 2/3 post-sound vs layer 5/6 control and layer 2/3 post-sound vs layer 5/6 post-sound), were found significantly different whereas the remaining three (layer 2/3 control vs layer 5/6 control, layer 2/3 control vs layer 5/6 post-sound and layer 5/6 control vs layer 5/6 post-sound) were found statistically non-significant at the same confidence level. These results were also comparable to results obtained when the speaker was placed on the sides of the animal. Together, these results displayed the extended plastic nature of layer 2/3 neurons over layer 5/6 neurons and confirmed the independent response change when the position of sound source was modified.

Sound impacts bandwidth of supra- and infra-granular neurons

The sharpness of orientation selectivity can be evaluated by measuring the bandwidth at half height of the orientation Gaussian tuning curve (Ringach *et al.*, 2002; Moore *et al.*, 2005). With this approach, we compared the tuning bandwidth of all neurons in either layer in control and post-sound conditions. The graphs shown in Figure 6 are a compilation of bandwidth analyses on layer 2/3 and layer 5/6 neurons. Figure 6 A shows results for layer 2/3 neurons (N = 60). Overall, the tuning bandwidth at half magnitude (FWHM: full width at half magnitude) was found to be slightly enlarged at post-sound condition but not significantly different (Wilcoxon matched-pairs signed rank test, P-value = 0.0663). The increase of bandwidth of a neuron indicates broadening of selectivity for range of orientations signifying a large

contribution of flank orientations in the overall tuning of the neuron. Such an increase in bandwidth strongly proposes that sound repetition induces the development of a different preferred orientation of the same neuron with a broader tuning curve. This effect can be further understood by relating the results observed in Figure 4 A where values of orientation preference for layer 2/3 cells held a bias towards the horizontal orientations post-sound application. It appears as if the groups of neurons recorded from different sites in layer 2/3 were affected similarly on the application of sound and made all superficial layer neurons respond towards the sound in the same way. Similarly, in Figure 6 B, layer 5/6 cells (N = 80) also showed a similar increment in the bandwidth responses that was found to be statistically significant (Wilcoxon matched-pairs signed rank test, P-value = 0.0697). The means for layer 2/3 and layer 5/6 were 24.07 ± 3.58 and 56.13 ± 4.60 respectively and were tested to be significantly different (Mann-Whitney test, P-value<0.001). These results suggested that though both layers displayed similar behavior following the sound stimulus nonetheless layer 5/6 cells exhibited larger shifts of the peak of the tuning curves in comparison with layer 2/3.

Finally, the mean values of neurons' bandwidths were compared with each other in both layers (Figure 6 C). All groups were compared with each other using One-way ANOVA. The means (means ± SEM) for the mentioned four data sets were 17.53 ± 2.29, 28.14 ± 3.59, 22.74 ± 2.73 and 72.52 ± 4.38 respectively. Two out of six groups, (layer 2/3 post-sound vs layer 5/6 post-sound and layer 5/6 control vs layer 5/6 post-sound), were found significantly different (Tukey's multiple post comparison test), whereas others (layer 2/3 control vs layer 2/3 post-sound and layer 2/3 control vs layer 5/6 control) were found statistically non-significant at the same confidence level. In summary, these results showed a global deviation of layer 5/6 cells with higher means of bandwidths.

Orientation Selectivity Index (OSI)

In line with the previous reports (Dragoi *et al.*, 2001; Ringach *et al.*, 2002; Atallah *et al.*, 2012; Denman & Contreras, 2014) neurons having an OSI superior or equal to 0.4 can be classified as sharply tuned cells. In this investigation OSI values for all cells have been pooled to generate the figure. Figure 7 A and 7 B

shows results for layer 2/3 neurons (N = 124) and layer 5/6 neurons (N = 115) respectively. Overall, the OSI remained same at for either layer at both control and post-sound conditions yet the deviation for layer 2/3 neurons (Wilcoxon matched-pairs signed rank test, P-value<0.001) was found more than layer 5/6 neurons (Wilcoxon matched-pairs signed rank test, P-value = 0.0216). Thus, layer 5/6 experience more dispersed evoked response towards all presented orientations (Figure 7 B). The comparison between all groups (using Tukey's multiple post comparison test) showed that layer 5/6 neurons experienced a decline in selectivity to preferred orientation (Figure 7 C). Two out of six groups (control layer 5/6 vs post-sound layer 2/3, control layer 2/3 vs post-sound layer 2/3) were found significantly different whereas remaining four groups were found to be non-significant. These results also correspond to our results from bandwidth data. The broadening of tuning curves after the imposition of sound lead to decrease in mean OSI.

Response change index (RCI): Response modulation comparison between orientations

As described in methods section the modulation of response magnitude was calculated for all cells and for all applied oriented gratings. The values for layer 2/3 (N = 124) and layer 5/6 (N = 115) cells have been pooled to generate the figure. Results are compiled in Figure 8. The means RCI (mean ± SEM) of all layer 2/3 and layer 5/6 neurons (Figure 8 A) were -0.03435 ± 0.02 and 0.03098 ± 0.02 and were found statistically non-significant (Mann Whitney Test, P-value = 0.0682). In layer 2/3, responses fluctuated roughly with the same magnitude for all tested orientations. The differences between all possible pairs among all orientations were measured by one-way ANOVA and Tukey's multiple comparison test was applied to compare variances among means. The differences between all orientations in layer 2/3 were found non-significant (Figure 8 B). Interestingly, in layer 5/6 (Figure 8 C) the largest RCI was calculated for orientations close to the vertical axis (recall cells in both layers were recorded simultaneously). If we analyze closely, RCI regularly declined to become negligible in both directions as we go away from vertical to horizontal orientations. Only five (0° vs 90°, 22° vs 90°, 45° vs 90°, 90 vs 135° and 90° vs 157°) out of twenty-eight groups tested significantly different. This analysis, however, unveils another exciting observation. When RCI was analyzed at individual orientations, we found that, in supragranular

layers, the firing rate decreased for most orientations whereas in infragranular an opposite effect was observed. Nevertheless, the overall response variation is balanced (refer to Figure 8 A). Altogether, layer 2/3 neurons experienced response suppression and layer 5/6 neurons experienced response enhancement. Finally, the striking inverse response modification of layer 2/3 and layer 5/6 neurons indicated that supra- and infra-granular layers behave differently towards the identical stimuli conditions and it appears cells of both layers behave in independent fashion to process information. Also, dynamic changes in excitation and inhibition during the presentation of sound may be responsible for bringing out the prominent opposite behavior of neurons in the V1 columns.

Discussion

The present study aimed to investigate the responses of visual neurons of V1 when stimulated by a repetitive auditory stimulus whose frequency and power varied cyclically presumably driving many putative synaptic inputs. The investigation revealed three main findings. First, a surprisingly novel and the most important result, we observed shifts in the peaks of orientation tuning curves in cat's supra -and infragranular layers implying a novel orientation selectivity. Second, superficial and deeper layers neurons seemed to behave independently although both were recorded from the same columns at the same time. Moreover, occasionally, cells in both layers shifted in opposite directions. Third, neurons in infra-granular layer 5/6 exhibited larger shifts of their orientation selectivity than the layer 2/3 neurons. Collectively, these findings suggest that neurons in the primary visual cortex (V1) are not merely extractors of visual features but even respond well to non-visual information (Shuler & Bear, 2006; Keller *et al.*, 2012; Poort *et al.*, 2015).

Supramodal nature and cross-modal plasticity in the cortex

Our results exclusively put forward a new case of audio-visual interactions, and further amplify the observations made by previous investigations in cross-modal plasticity. Unlike the relatively slight

modulation of response in terms of firing rate of neurons detected in previous investigations (Iurilli *et al.*, 2012; Ibrahim *et al.*, 2016), we observed a much more intense response-change in our data, wherein V1 neurons experienced a complete shift in their orientation preference. This kind of modification was earlier reported in literature related to adaptation studies where neurons were only imposed with an adapting orientation (visual stimulus) and acquired new preferred selectivity. These visual adaptation protocols pertain to the classical flow of information involving LGN to the input layer 4 of the V1 and then to layer 2/3 and finally to the layer 5/6. In the current case, similar results were obtained. Indeed, in this case, it is the application of sound for several minutes that induced neurons to acquire a new preferred orientation even when exposed to a non-visual input. Interestingly, the present study involves a non-geniculate direct pathway. Comparing the two effects, it is indeed intriguing how the cortex may display various possible avenues to acquire the outside information. From our finding, the set of questions that may enthuse the brain are: is this because the perceived sound stimulus by the animal generates a visual format of the sound stimulus thus eliciting an intense response in the visual neurons? Is it because the visual cortex can inherently respond to an auditory stimulus since it is intrinsically supramodal in nature? Is it that cortex responds to the context of presented sound stimuli? Alternatively, is it a combination of all these possibilities? Though the principle underlying such interactions has not been fully discovered yet, the most suitable explanation that fits in with the results is the combination of cross-modal plastic mechanisms and supramodal nature of the visual cortex may explain the results. It's that the visual cortex is a stimulus-driven structure, therefore it exhibits unique response pattern towards different protocols and stimuli. Perhaps, this ability is induced during developmental stages and evolved with experience. It seems likely that cross-modal interactions are recruited more often in early blinds or congenital blinds because there is an urgent need for another sensory modality to take over the responsibility to trigger processing at early stages and then also employ the visual cortex to respond in full capacity. In this case, a reorganization of the cortex is generally noted for a recalibration of the sensory system. In the present study, healthy animals were monocularly stimulated. Therefore the possibility undergoing a supramodal mechanism supported by a cross-modal communication between sensory structures seems more

reasonable. It is hypothesized that, upon sensory activation, the visual cortex relies on the abstract representation of the sensory stimuli regardless of the sensory modality. Alternatively, upon triggering by a sound stimulus, both visual and auditory cortices are engaged cross-modally and both approaches exist together. A related line of thought by Muckli and colleagues (Muckli *et al.*, 2015) further highlights that a significant source of information lies in the context of the stimuli. Any sensory stimulus involving a feature can potentially embody the global features of the stimuli that are enough to trigger a complex scene representation of the same sound stimulus in the visual cortex (Bar, 2004; Oliva & Torralba, 2007), especially when presented for a prolonged duration. Raw signals may carry information about the overall structure of the scene in the form of contours, and this rough representation can help to segment the scene and boost the recognition process within the scene associated with that specific sound. It is thought-provoking, considering the intense interconnectivity within and between different sensory areas of the cortex. Although these effects have been discussed mainly from imaging studies on humans, the underlying principle reasonably explains our data (Vogels, 1999; Muckli *et al.*, 2005; Vetter *et al.*, 2014; Muckli *et al.*, 2015).

Inhibitory mechanisms

Recent studies have suggested that sound modulates light responses by impacting inhibitory neurons in the V1 (Iurilli *et al.*, 2012; Kayser & Remedios, 2012; Pluta *et al.*, 2015; Ibrahim *et al.*, 2016). A very recent report (Deneux *et al.*, 2018) has revealed that the auditory cortex neurons project to the V1 inhibitory neurons in the superficial layers, especially layer 1. These interneurons act as initiating points and as a passage for a cross-modal stream that recruits a suppressive approach of processing. This specific pathway is activated precisely in response to only non-visual inputs (Deneux *et al.*, 2018). Further, they found that specific interneurons that generate inhibition simultaneously conceal the excitatory drive from the auditory cortex to V1 (Deneux *et al.*, 2018). They reported that the observed inhibitory mechanism observed originated in a dark setup, and these results could be applied to the current investigation since the experiments were also performed in similar conditions: in darkness. The most important result from

their study unveiled that only the inhibitory neurons in superficial layer 1 of the primary visual cortex consist of a subpopulation of GABAergic neurons that are implicated in sound-induced inhibition. Further, authors added that these interneurons process context-dependent information and produce inhibitions upon meeting the action potentials travelling from A1 (Deneux *et al.*, 2018). In addition, it has been (Iurilli *et al.*, 2012; Ibrahim *et al.*, 2016) shown that sound excites GABAergic cells in V1 which in turn hyperpolarize pyramidal neurons and suppress evoked light responses. Hyperpolarizing pyramidal cells may lessen their excitation upon interaction with inhibitory cells and in turn, further weaken cross-orientation inhibition via a disinhibition process. Such steps may lead to changing of preferred orientation into another optimal orientation that result to shifts of selectivity. Therefore, this could explain how neurons maintain inhibition in the visual cortex for the entire sound stimulation process of 12 minutes. Henceforth, in most cases, audio-visual interactions are disclosed by modulations of the magnitude of evoked responses to visual targets in the presence of sound. On similar lines, it has been hypothesized that sound exerts a divisive or additive influence, resulting in a decline or enhancement of light responses (Pluta *et al.*, 2015).

Layer 2/3 and layer 5/6 neurons change orientation preferences

In line with the previous studies in visual adaptation, many authors have described shifts of optimal orientation tuning or changes in orientation selectivity after a short (less than a minute) (Dragoi *et al.*, 2000) or long light adaptation (Ghisovan *et al.*, 2008, 2009; Bachatene *et al.*, 2012b; Bachatene *et al.*, 2013; Bachatene *et al.*, 2015; Chanauria *et al.*, 2016) (several minutes). Usually, the protocol requires the frequent or continued application of a non-preferred property of the adapter such as orientation. In the above experiments, the peak of the orientation tuning curve is displaced either toward (attractive) or away (repulsive) from the adapting orientation. In all cases, such protocol results in the emergence of a novel orientation selectivity. It has also been demonstrated in our previous studies (Chanauria *et al.*, 2016) that layer 2/3 and layer 5/6 neurons work in parallel towards the adapter orientation and thus neurons in both layers can attain new selectivity following adaptation. Neurons undergo a push-pull mechanism

(Bachatene *et al.*, 2012b; Bachatene *et al.*, 2013; Bachatene *et al.*, 2015; Chanauria *et al.*, 2016) that is characterized by the decrease and increase of the firing rates at the initially preferred and the adapting orientation (newly acquired) respectively.

In the current investigation, the non-preferred stimulus traditionally referred to as visual adapter, is absent and is replaced by exposure to a sound stimulus imposed in seclusion for several minutes uninterruptedly, wherein responses of individual visual neurons are recorded before and after the sound application and then compared. Results revealed that such presentation of sound not only modulates visual responses but entirely shifts the orientation tuning curves of individual visual neurons in supra and infragranular layers of area 17 of cats. Consequently, sound seemed to exert distinctive effects in addition to the global modulatory influence. As orientation selectivity is shaped at the cortical level, thanks to aligned thalamic inputs upon the cortical recipient neurons, the changes of orientation selectivity are unlikely to happen at thalamic levels, where cells have mostly concentric receptive field (although some units may exhibit a slight orientation bias). Further, we found populations of neurons (layer 2/3 and layer 5/6) exhibiting enhanced or diminished responses while the overall response of the population remained balanced (Figure 7A). Especially, at 90° orientation, a clear enhancement of response is noticed whereas suppression in layer 2/3 neurons. Layer 5/6 cells experienced an increase of excitation.

It has been noted that short duration sounds produce weak visual responses (Brady, 2011; Deneux *et al.*, 2018). Yet, repeated presentation of the sound stimulus for a prolonged duration may be accountable for eliciting stronger responses in V1. Undoubtedly, the repeated stimulation aids in crossing threshold and generating the required strength of interaction as substantial visual input reaches the V1. This kind of mechanism can logically happen in layer 2/3 where pyramidal neurons receive direct inputs from auditory cortex, as 12 min time is enough to encode the raw embedded visual information within the audio stimulus. The underlying principle explained above can certainly be applied in the current scenario. The bias we observed may perhaps be a consequence of such a process, and that is why we observe an evident response bias towards horizontal orientation for layer 2/3 neurons but not in layer 5/6. Also, this predisposition could be inherently induced because of the property of the sound itself. It has been known

for many years now that visual cortex is a stimulus-driven structure (Doron *et al.*, 2002; Izraeli *et al.*, 2002; Piche *et al.*, 2007; Chabot *et al.*, 2008). The non-visual information in the stimulus can transmit from non-visual sensory structures to visual cortex by direct corticoccipital pathways and circumvent the higher order cortex. Further, in this situation, the nonvisual signals do not undergo a modulation but only translate the stimulus-driven information. Xu and co-authors (Xu *et al.*, 2012) suggested that functional mixing of inputs from two different sources could allow for facilitative non-linear interactions within individual dendrites that may lead to the bias towards horizontal orientations. This non-linearity may clarify a preference towards the horizontal orientations. Another important revelation from a previous study (Deneux *et al.*, 2018) suggests that the increasing intensity of sound strengthens the neuronal response. The intensity of the stimulus we used was kept same for the 3s, and the same 3s time was repeated throughout 12 min, therefore, with every repetition the representation of the information embedded in sound became dominant, consequently leading to a change of selectivity and not just a modulation of firing rate. However, neuronal firing shows a non-linear trend towards the duration of the sound presented (Xu *et al.*, 2012).

Layers behave as separate compartments

Our results also show that the application of sound differentially affected the layers 2/3 and 5/6, thereby also reconfiguring the layout of orientation maps in the V1. Ibrahim and co-authors (Ibrahim *et al.*, 2016) demonstrated that layer 2/3 neurons get suppressed by the A1 signals, a result that we found too. Layer 2/3 neurons keep receiving the information for 12 min and presumably the intensity of the inhibitory drive increases with the duration of stimulation. In this scenario, another feedback drive initiates in A1 and interacts with layer 5/6 neurons that further maintain the influence on layer 2/3 cells (Fritz *et al.*, 2003; Muckli & Petro, 2013; Vetter *et al.*, 2014; Muckli *et al.*, 2015; Ibrahim *et al.*, 2016). Therefore, it appears that the layer 2/3 receives extreme inhibition whereas layer 5/6 neurons experience more excitation. The application of sound differentially affected the layers 2/3 and 5/6, thereby also reconfiguring the layout of orientation maps in the V1.

It has been demonstrated that fibers emerging from auditory cortices activate mostly GABAergic inhibitory cells which in turn hyperpolarize pyramidal cells in both infra- and supra-granular layers in the visual cortex (Ibrahim *et al.*, 2016). There are direct and indirect connections arising from V1 and ending at different areas in the cortex, almost covering the entire cortex and making it reciprocally interconnected (Petro *et al.*, 2013; Petro *et al.*, 2017). As electrodes were introduced orthogonally in area 17, presuming each recording site in layers 2/3 and 5/6 was in the same orientation column, the dual projections of neurons onto each other in supra and infragranular layers may elucidate shifts of the peak of tuning curves in the opposite direction (see example tuning curve).

Conclusion

Undeterred by the traditional view of sensory processing that restricts the merging of sensory information only to higher association cortices, latest reports suggest that the early visual cortex is also involved in the integration of multimodal information. Nevertheless, a crucial and detailed inspection is required to fully fathom the mechanisms of cross-modal integration in primary sensory areas, especially the primary visual cortex. Together, our data demonstrated that visual cortical neurons can respond to sound stimulations in the absence of any visual inputs in a strong manner that leads them to undergo an alteration of selectivity. Further, understanding cross-modal plasticity employs specific pathways (perhaps, hitherto unknown) within and between sensory areas to process diverse inputs and response towards outside environment can be varied. A model of possible mechanisms underlying our observations have been displayed as Figure 9. The model has been adopted and suitably modified from papers already cited in the text.

Legends

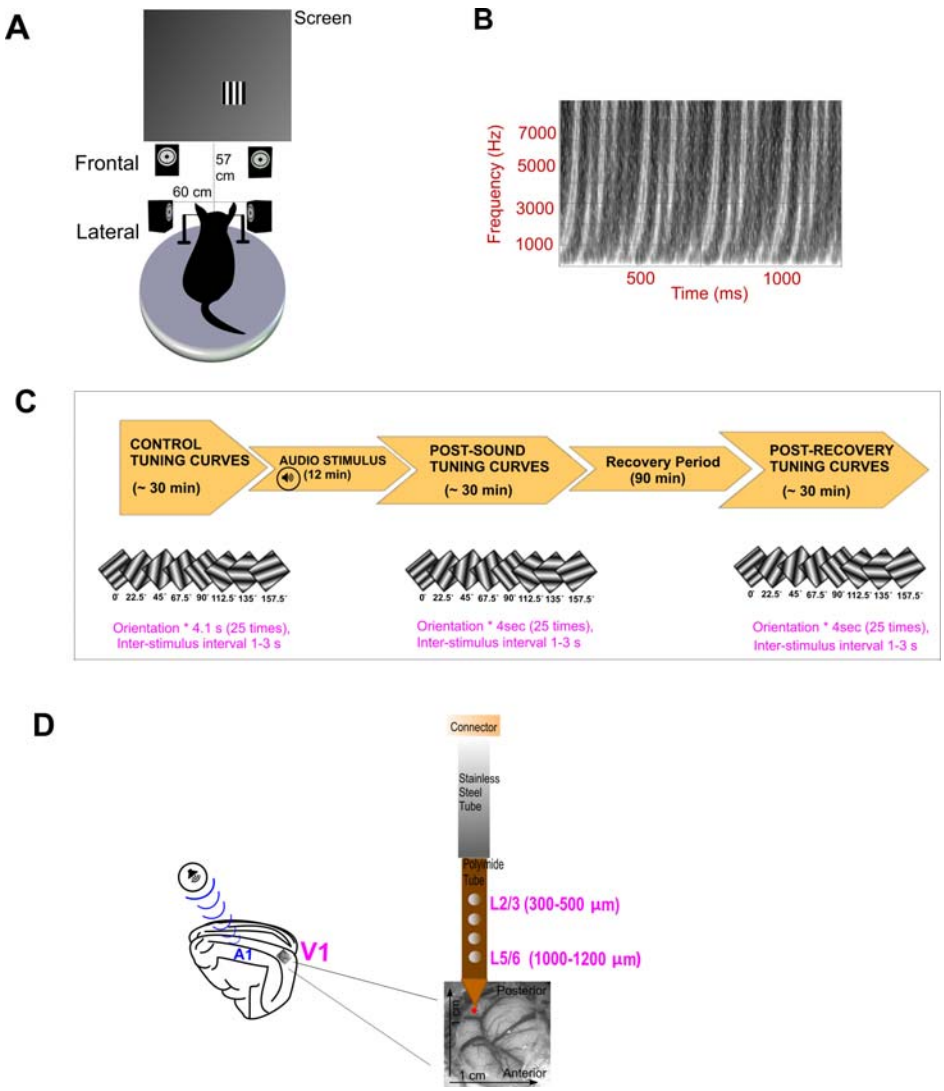

Figure 1

Experimental set up of stimulation, neuronal recordings and sound stimulus (A) Cartoon of the anesthetized cat fixed on the stereotaxic apparatus. Visual stimulus (shown as black and white gratings) was presented inside the receptive fields of test neurons. The sound stimulus was delivered by a pair of speakers occasionally placed frontal or lateral to the axis of the animal (B) The spectrogram of the sound stimulus is displayed. The spectrogram shows that sound stimulus was played in a constant frequency modulation (FM) pattern. (C) A pictorial representation of the steps followed during the protocol. Two types of stimulus were applied: Visual and auditory. Visual stimuli (sine-wave drifting oriented-gratings)

were presented in a random order. Each orientation was presented 25 times and each trial lasted 4 s with a 1–3 ms inter-stimulus interval followed by presentation of the sound stimulus for 12 min. Then, the same set of visual stimuli was presented to the animal again in a random order. A recovery period of 90 min was offered after which the gratings were presented again randomly (D) Illustration of the electrode used to record neuronal activity. Neurons were recorded using multichannel depth electrode from 300-500 µm, and 1000-1200 µm from the primary visual cortex (V1) /area 17 before and after auditory stimulation.

Figure 2

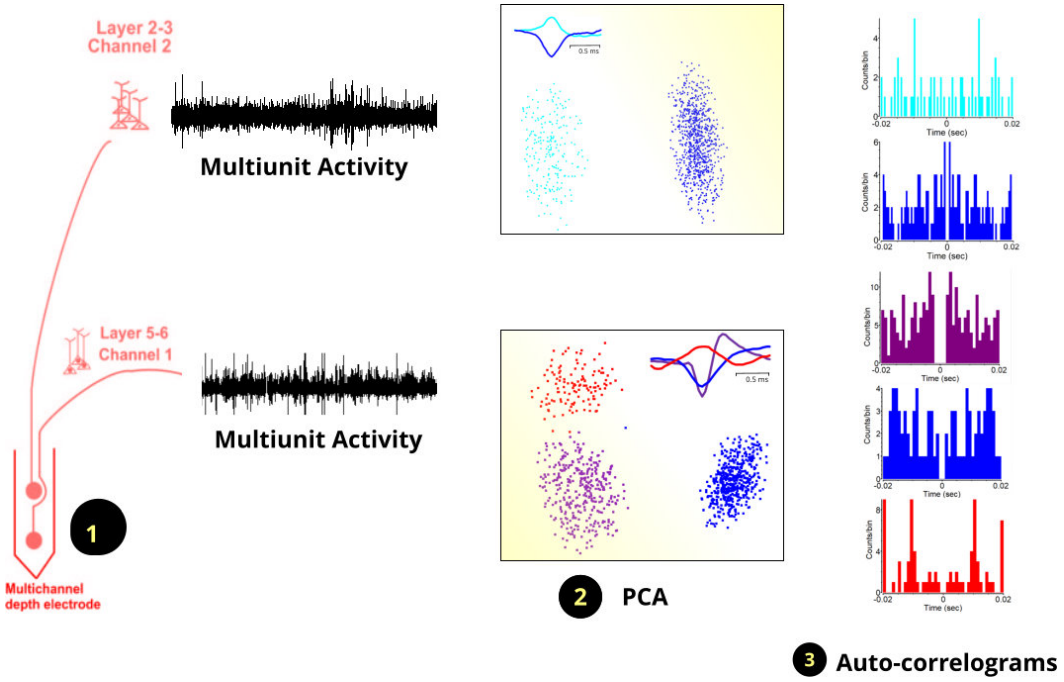

An example of the spike sorting process for isolation of single units is exhibited. Part 1 displays that the neurons have been recorded simultaneously from layer 2/3 and layer 5/6 of the V1. Multiunit activity from both layers is also displayed alongside. Part 2 shows the principal component analysis of the dissociated waveforms. The superimposed average waveforms of dissociated spikes from multi-unit recordings have

also been shown. Part 3 displays the auto-correlograms for the separated single units. No events at zero represent the refractory period of neuron that confirms the individuality of each neuron.

Figure 3

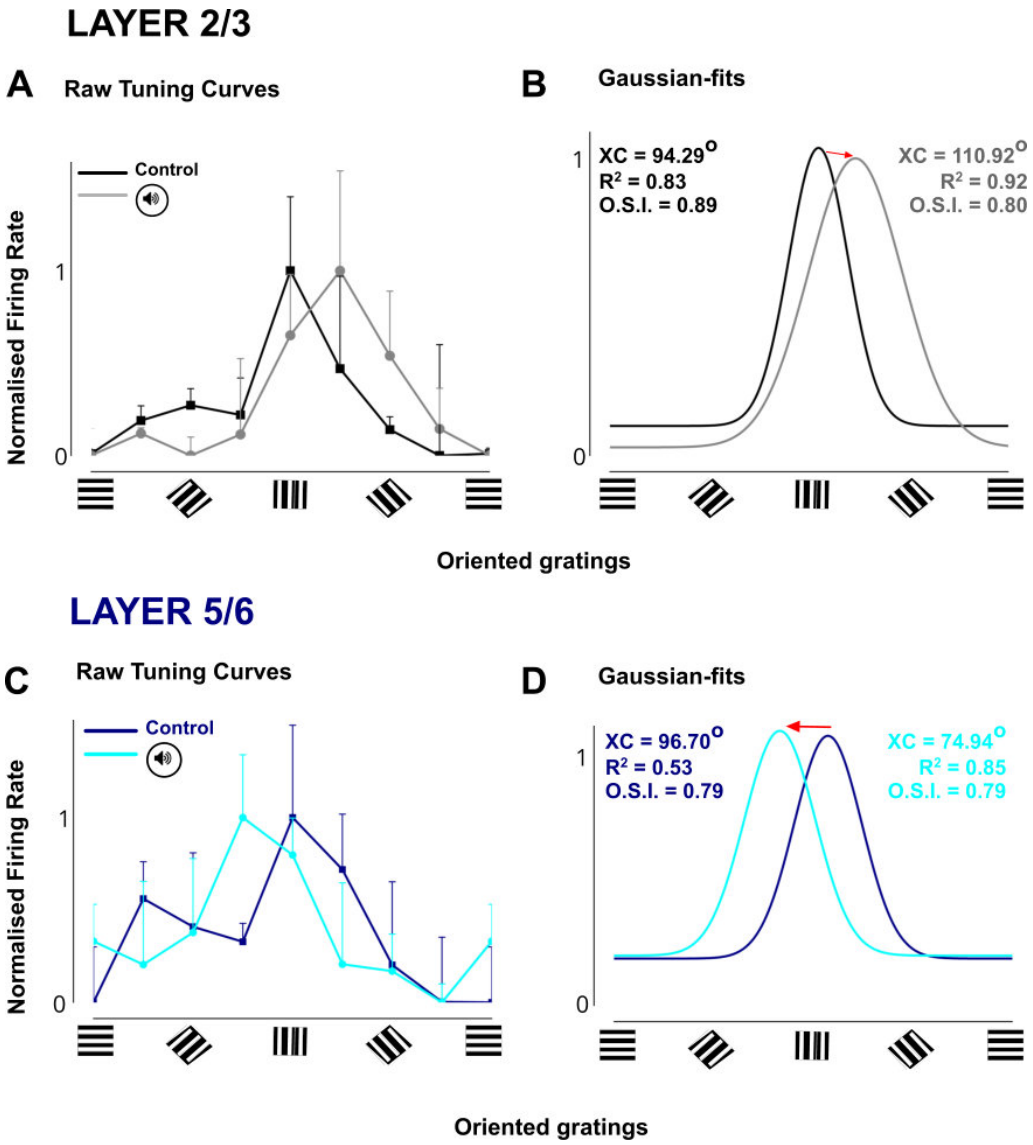

A typical example of a shift of orientation tuning peak. The figure represents a pair of layer 2/3 and layer 5/6 neuron recorded simultaneously during the protocol. The bars signify standard error of the mean (mean ± SEM) over 25 trials at each presented oriented grating. The direction of shift is highlighted by an arrow (A) Raw orientation tuning values were compared for layer 2/3 neuron at control and post-sound conditions. A clear change in selectivity can be observed (B) To deduce the exact values of orientation tuning raw values were fitted using the Gauss function. An overlap of the initially preferred and the new selectivity has been depicted along with the XC, R^2 and OSI values. (C) Raw tuning curves of layer 5/6 neuron at control and post-sound conditions are displayed (D) Gaussian fitted tuning curves for layer 5/6 neuron over raw data is shown. The values of XC, R^2 and OSI are also displayed along.

Figure 4

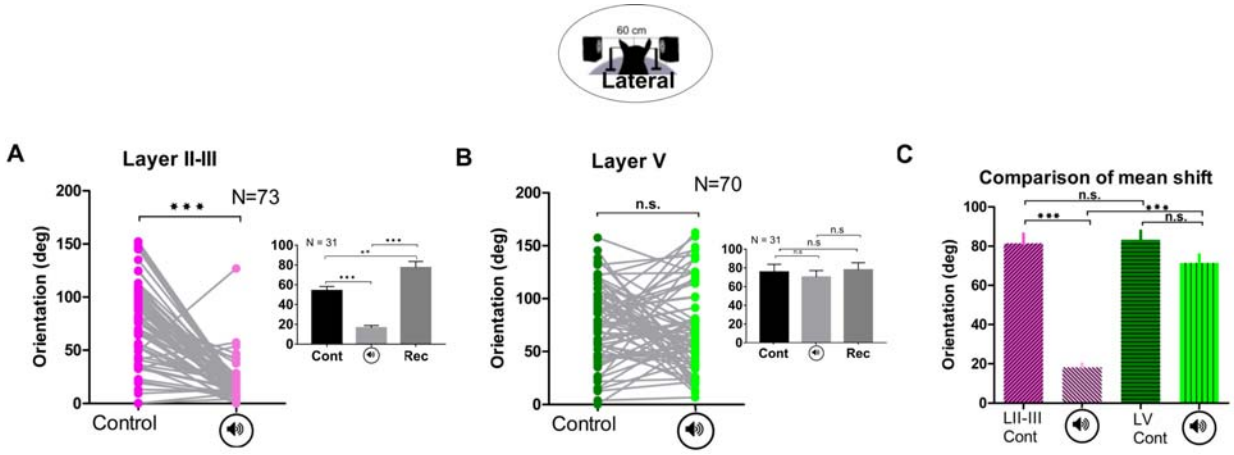

Acoustic stimulation results in modification of orientation preference and variation of shift-magnitudes in V1 orientation columns. In this figure, we show shift magnitudes for neurons in either layer. Connected points represent individual cell. Cells' shift magnitude data did not pass the Shapiro-Wilk normality test, and consequently, non-parametric statistical approach was followed. The significant differences are indicated by a solid black line above each plot. The graphs A-C comprise of the obtained values of orientation selectivities when speakers were placed on either side of the animal with respect to the fixation

axis of the animal (A) A plot of orientation tuning values for layer 2/3 neurons (N=73), at control and post-sound presentation conditions is displayed (Wilcoxon matched-pairs signed rank test, P value <0.0001). In the insert on the right side, the histogram in grey and black shows the comparison of orientation selectivity values at control, postsound and recovery conditions (Wilcoxon matched-pairs signed rank test: Cont-Postsound, P value <0.0001; Control-Recovery, P value <0.0047; Postsound-Recovery, P value <0.0001) (B) A plot of orientation tuning values for layer 5/6 neurons (N=70) is displayed for control and post-sound conditions (Wilcoxon matched-pairs signed rank test: Cont-Postsound, P value = 0.6152; Control-Recovery, P value = 0.4487; Postsound-Recovery, P value = 0.8325). The difference between the means of control and recovery orientation tuning values are also shown as the small histogram on the right side of the main figure (Paired t-test, P value = 0.8276) (C) Graph showing mean of amplitudes at control and post-sound condition. All four groups layer 2/3 control, layer 2/3 post-sound, layer 5/6 control and layer 5/6 post-sound were compared in this analysis using One-way ANOVA. The means (mean ± SEM) for the mentioned four data sets were 81.41 ± 4.952, 18.15 ±1.882, 83.33 ± 4.566 and 71.38 ± 4.332 respectively. Further, with the help of Tukey's multiple post comparison test, the differences between datasets were calculated. Out of all possible groups, three groups (layer 2/3 control vs layer 2/3 post-sound, layer 2/3 post-sound vs layer 5/6 control and layer 2/3 post-sound vs layer 5/6 post-sound) tested significant, whereas the remaining three groups (layer 2/3 control vs layer 5/6 control, layer 2/3 control vs layer 5/6 post-sound and layer 5/6 control vs layer 5/6 post-sound) were found statistically non-significant the same confidence level.

Figure 5

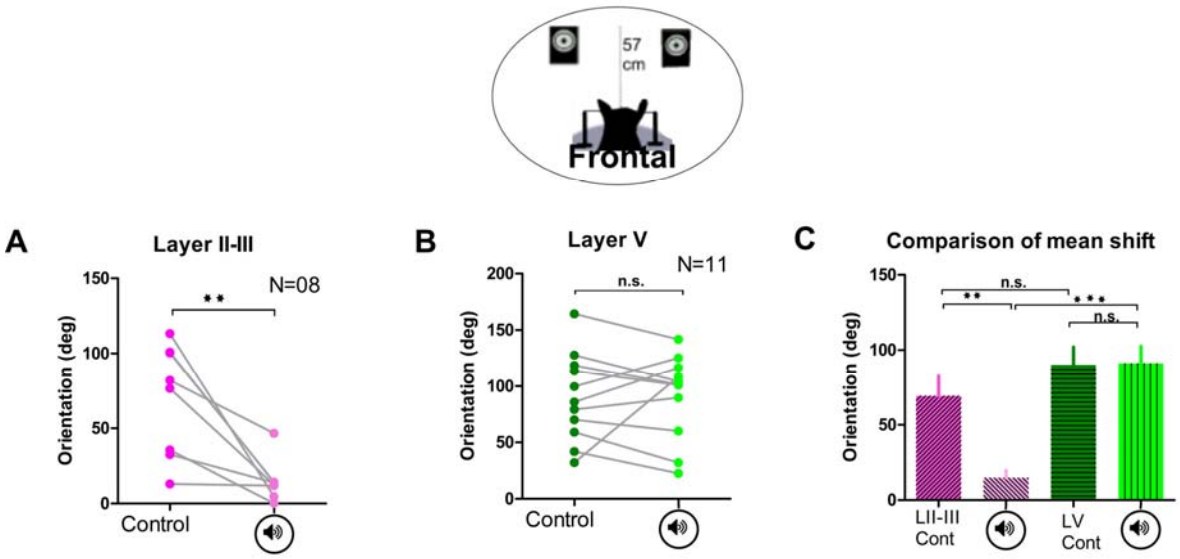

The graphs A-C show results when the speakers were positioned in front of the animal. A non-parametric statistical approach was followed since the data did not pass the normality test. Connected points represent individual cell (A) Orientation tuning values for layer 2/3 neurons (N = 8) were plotted at both conditions and the difference was found significant (Wilcoxon matched-pairs signed rank test, P value = 0.0078) (B) Orientation tuning values of layer 5/6 neurons (N = 11) are displayed in the graph (Wilcoxon matched-pairs signed rank test, P-value = 0.8984) (C) Histogram of mean of amplitudes at control and post-sound conditions. The four groups (layer 2/3 control and post sound and layer 5/6 control and post-sound) were compared using One-way ANOVA. The means (mean ± SEM) for the mentioned four data sets were 69.34 ± 13.21, 14.79 ± 4.908, 90.22 ± 11.91 and 91.24 ± 11.38 respectively. Further, using Tukey's multiple post comparison test, the differences between all groups were calculated. Three out of six groups (layer 2/3 control vs layer 2/3 post-sound, layer 2/3 post-sound vs layer 5/6 control and layer 2/3 post-sound vs layer 5/6 post-sound) were statistically different whereas the remaining three groups (layer 2/3 control vs layer 5/6 control, layer 2/3 control vs layer 5/6 post-sound and layer 5/6 control vs layer 5/6 post-sound) were found statistically non-significant at the same confidence level.

Figure 6

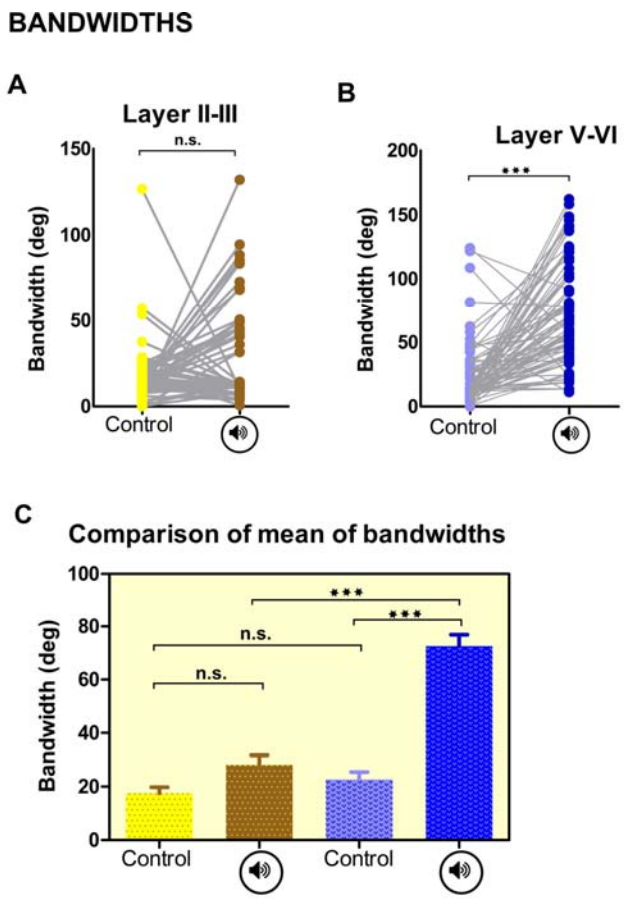

The sharpness of orientation selectivity. A non-parametric statistical approach was followed to measure significance between data sets. Connected points represent individual cell. (A) The numerical values of bandwidths were plotted for layer 2/3 cells (N = 60) at control and post-sound conditions (Wilcoxon matched-pairs signed rank test, P-value = 0.0663) (B) A similar plot of bandwidth values for layer 5/6 neurons (N=80) is shown (Wilcoxon matched-pairs signed rank test, P-value = 0.0697) (C) Graph showing mean of bandwidths at control and post-sound condition. All four groups (layer 2/3 control, layer 2/3 post-sound, layer 5/6 control and layer 5/6 post-sound) were compared in this analysis using One-way ANOVA. The means (mean ± SEM) for the mentioned four data sets were 17.53 ± 2.293, 28.14 ± 3.595, 22.74 ± 2.736 and 72.52 ± 4.389 respectively. Further, with the help of Tukey's multiple post comparison tests the differences between all four datasets were calculated. Three groups (layer 2/3 control vs layer 5/6 post-sound, layer 2/3 post-sound vs layer 5/6 post-sound and layer 5/6 control vs layer 5/6 post-sound)

were found significantly different whereas remaining groups (layer 2/3 control vs layer 2/3 post-sound, layer 2/3 control vs layer 5/6 control and layer 2/3 post-sound vs layer 5/6 control) tested statistically non-significant at the same confidence level.

Figure 7

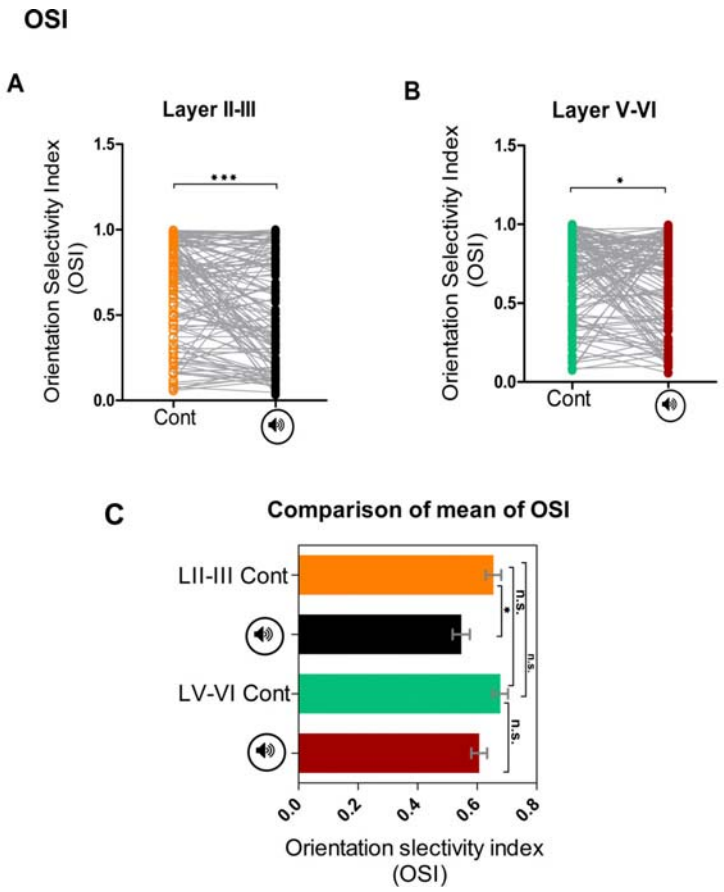

Orientation Selectivity Index (OSI) A non-parametric method has been adopted to measure differences between different populations. Connected points represent individual cell. (A) OSI values calculated for layer 2/3 neurons (N = 124) at control and post-sound conditions have been displayed and were found significantly different (Wilcoxon matched-pairs signed rank test, P value < 0.0001) (B) Similar symbol and line plot are also shown for layer 5/6 neurons (N = 115) at both circumstances (Wilcoxon matched-pairs signed rank test, P-value = 0.0216) (C) The values of OSI from either layer for both conditions was

compared using One-way ANOVA. Only two groups tested statistically different for means (control layer 5/6 vs post-sound layer 2/3 and post-sound layer 2/3 and control layer 2/3) whereas remaining groups were not found different at any significance level.

Figure 8

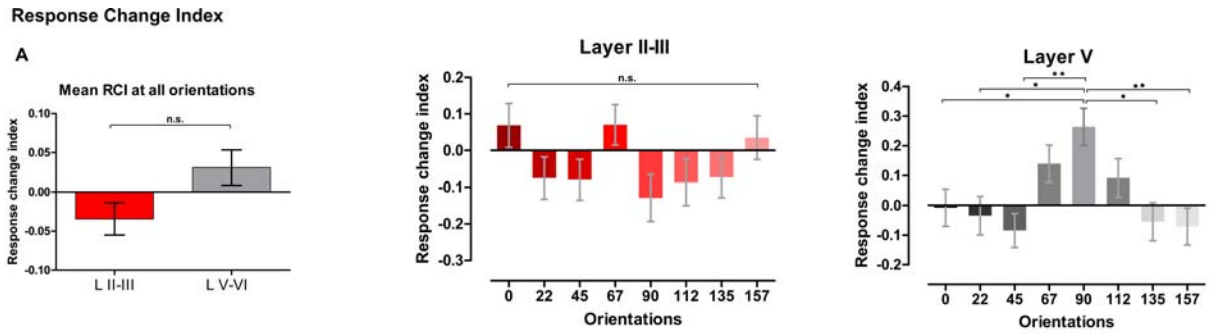

Response Change Index (RCI). A non-parametric method was opted for statistical validations (A) Histogram showing mean of RCI of all test neurons in either layer at all presented orientations (0° - 157.5°, separated by 22. 5°). The mean RCI (mean ± SEM) of all layer 2/3 and layer 5/6 neurons were -0.03435 ± 0.02054 and 0.03098 ± 0.02241 and statistically non-significant (Mann Whitney Test, P-value = 0.0682) (B) A graph showing histograms of RCI at different orientations for layer 2/3 cells. The differences between all possible pairs among all orientations were measured by one-way ANOVA and Tukey's multiple comparison test. (C) A similar analysis was done on layer 5/6 neurons, and the histogram was generated. Five groups out of all possible paired comparisons (0° vs 90°, 22° vs 90°, 45° vs 90°, 90° vs 135°and 90° vs 157.5°) tested significantly different whereas, for rest of the groups, the mean of RCI was not significantly different.

Figure 9

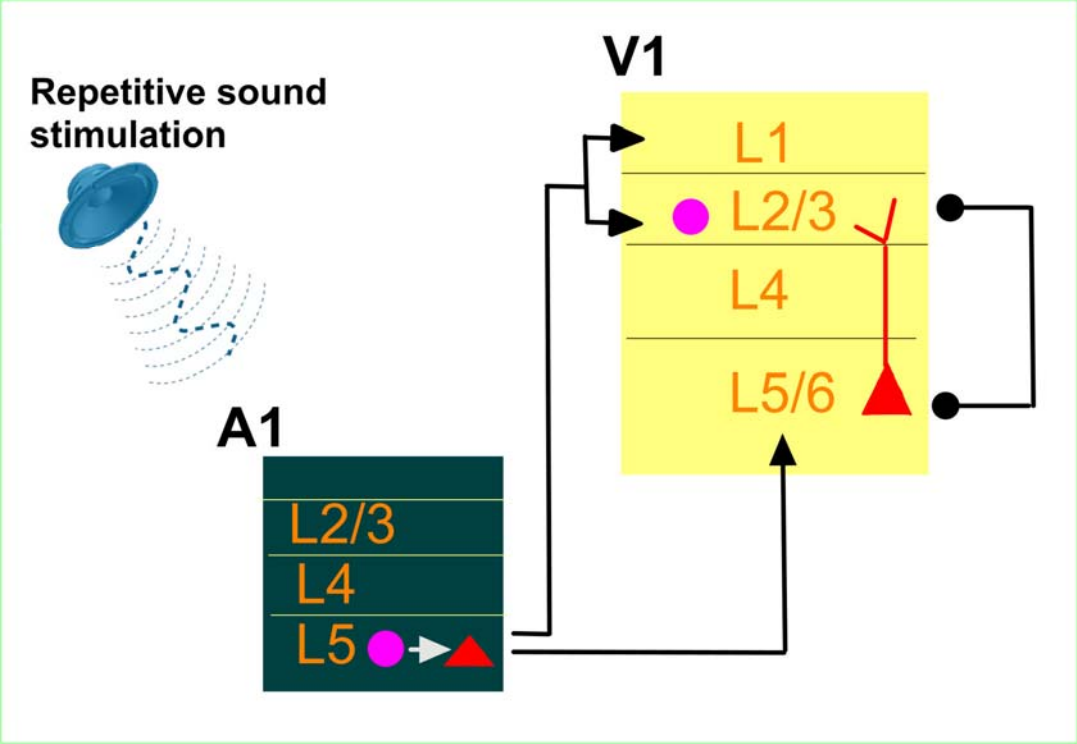

A model of possible neural mechanisms underlying the modification of the orientation tunings of individual neurons in supra- and infra-granular layers in the V1 cortical column. The model has been adopted from different studies that were discussed throughout the text. On the onset of sound, A1 gets stimulated and triggers projections directly on superficial layers of the V1. A1 projections recruit GABAergic cells in layer 1 and 2/3 of V1 and generate inhibition within this interaction. During this process, a disinhibitory mechanism within and between 2/3 cells and layer 5/6 cells initiates wherein neurons in both layers project onto each other and consequently inhibit each other. In another case, auditory cortex might directly project on layer 5/6 of the V1.

Acknowledgements:

This research was supported by NSERC Canada, Grant no. 6943. SM, VB and NC designed the experiments. NC, VB, LB and SC participated in the experiments. NC wrote the paper and analyzed the

data, JR greatly assisted with the optimization of the auditory stimulus, SM and JR contributed with comments that greatly improved the manuscript.

References:

Atallah BV, Bruns W, Carandini M & Scanziani M. (2012). Parvalbumin-expressing interneurons linearly transform cortical responses to visual stimuli. *Neuron* **73,** 159-170.

Bachatene L, Bharmauria V, Cattan S & Molotchnikoff S. (2013). Fluoxetine and serotonin facilitate attractive-adaptation-induced orientation plasticity in adult cat visual cortex. *Eur J Neurosci* **38,** 2065-2077.

Bachatene L, Bharmauria V, Cattan S, Rouat J & Molotchnikoff S. (2015). Reprogramming of orientation columns in visual cortex: a domino effect. *Sci Rep* **5,** 9436.

Bachatene L, Bharmauria V & Molotchnikoff S. (2012a). Adaptation and Neuronal Network in Visual Cortex.

Bachatene L, Bharmauria V, Rouat J & Molotchnikoff S. (2012b). Adaptation-induced plasticity and spike waveforms in cat visual cortex. *Neuroreport* **23,** 88-92.

Bar M. (2004). Visual objects in context. *Nat Rev Neurosci* **5,** 617-629.

Bardy C, Huang JY, Wang C, FitzGibbon T & Dreher B. (2006). 'Simplification' of responses of complex cells in cat striate cortex: suppressive surrounds and 'feedback' inactivation. *The Journal of physiology* **574,** 731-750.

Barlow HB, Blakemore C & Pettigrew JD. (1967). The neural mechanism of binocular depth discrimination. *The Journal of physiology* **193,** 327-342.

Bharmauria V, Bachatene L, Cattan S, Brodeur S, Chanauria N, Rouat J & Molotchnikoff S. (2016). Network-selectivity and stimulus-discrimination in the primary visual cortex: cell-assembly dynamics. *Eur J Neurosci* **43,** 204-219.

Bharmauria V, Bachatene L, Cattan S, Chanauria N, Rouat J & Molotchnikoff S. (2015). Stimulus-dependent augmented gamma oscillatory activity between the functionally connected cortical neurons in the primary visual cortex. *Eur J Neurosci* **41,** 1587-1596.

Brady D. (2011). *Mechanisms of Cross-Modal Refinement by Visual Experience*.

Budinger E, Heil P, Hess A & Scheich H. (2006). Multisensory processing via early cortical stages: Connections of the primary auditory cortical field with other sensory systems. *Neuroscience* **143,** 1065-1083.

Butler BE, Chabot N, Kral A & Lomber SG. (2017). Origins of thalamic and cortical projections to the posterior auditory field in congenitally deaf cats. *Hearing research* **343,** 118-127.

Chabot N, Charbonneau V, Laramee ME, Tremblay R, Boire D & Bronchti G. (2008). Subcortical auditory input to the primary visual cortex in anophthalmic mice. *Neuroscience letters* **433,** 129-134.

Chanauria N, Bharmauria V, Bachatene L, Cattan S, Rouat J & Molotchnikoff S. (2016). Comparative effects of adaptation on layers II-III and V-VI neurons in cat V1. *Eur J Neurosci* **44,** 3094-3104.

Clavagnier S, Falchier A & Kennedy H. (2004). Long-distance feedback projections to area V1: implications for multisensory integration, spatial awareness, and visual consciousness. *Cogn Affect Behav Neurosci* **4,** 117-126.

Clemo HR, Lomber SG & Meredith MA. (2017). Synaptic distribution and plasticity in primary auditory cortex (A1) exhibits laminar and cell-specific changes in the deaf. *Hearing research* **353,** 122-134.

Deneux T, Kempf A & Bathellier B. (2018). Context-dependent signaling of coincident auditory and visual events in primary visual cortex. *bioRxiv*.

Denman DJ & Contreras D. (2014). The structure of pairwise correlation in mouse primary visual cortex reveals functional organization in the absence of an orientation map. *Cereb Cortex* **24,** 2707-2720.

Doron NN, Ledoux JE & Semple MN. (2002). Redefining the tonotopic core of rat auditory cortex: physiological evidence for a posterior field. *The Journal of comparative neurology* **453,** 345-360.

Dragoi V, Rivadulla C & Sur M. (2001). Foci of orientation plasticity in visual cortex. *Nature* **411,** 80-86.

Dragoi V, Sharma J & Sur M. (2000). Adaptation-induced plasticity of orientation tuning in adult visual cortex. *Neuron* **28,** 287-298.

Falchier A, Clavagnier S, Barone P & Kennedy H. (2002). Anatomical evidence of multimodal integration in primate striate cortex. *J Neurosci* **22,** 5749-5759.

Foxe JJ & Schroeder CE. (2005). The case for feedforward multisensory convergence during early cortical processing. *Neuroreport* **16,** 419-423.

Frenkel MY, Sawtell NB, Diogo AC, Yoon B, Neve RL & Bear MF. (2006). Instructive effect of visual experience in mouse visual cortex. *Neuron* **51,** 339-349.

Fries P, Nikolic D & Singer W. (2007). The gamma cycle. *Trends Neurosci* **30,** 309-316.

Fritz J, Shamma S, Elhilali M & Klein D. (2003). Rapid task-related plasticity of spectrotemporal receptive fields in primary auditory cortex. *Nat Neurosci* **6,** 1216-1223.

Ghazanfar AA & Schroeder CE. (2006). Is neocortex essentially multisensory? *Trends Cogn Sci* **10,** 278-285.

Ghisovan N, Nemri A, Shumikhina S & Molotchnikoff S. (2008). Visual cells remember earlier applied target: plasticity of orientation selectivity. *PLoS One* **3,** e3689.

Ghisovan N, Nemri A, Shumikhina S & Molotchnikoff S. (2009). Long adaptation reveals mostly attractive shifts of orientation tuning in cat primary visual cortex. *Neuroscience* **164,** 1274-1283.

Gielen SC, Schmidt RA & Van den Heuvel PJ. (1983). On the nature of intersensory facilitation of reaction time. *Perception & psychophysics* **34,** 161-168.

Henry GH, Bishop PO, Tupper RM & Dreher B. (1973). Orientation specificity and response variability of cells in the striate cortex. *Vision Res* **13,** 1771-1779.

Hershenson M. (1962). Reaction time as a measure of intersensory facilitation. *Journal of experimental psychology* **63,** 289-293.

Ibrahim LA, Mesik L, Ji XY, Fang Q, Li HF, Li YT, Zingg B, Zhang LI & Tao HW. (2016). Cross-Modality Sharpening of Visual Cortical Processing through Layer-1-Mediated Inhibition and Disinhibition. *Neuron* **89,** 1031-1045.

Iurilli G, Ghezzi D, Olcese U, Lassi G, Nazzaro C, Tonini R, Tucci V, Benfenati F & Medini P. (2012). Sound-driven synaptic inhibition in primary visual cortex. *Neuron* **73,** 814-828.

Izraeli R, Koay G, Lamish M, Heicklen-Klein AJ, Heffner HE, Heffner RS & Wollberg Z. (2002). Cross-modal neuroplasticity in neonatally enucleated hamsters: structure, electrophysiology and behaviour. *Eur J Neurosci* **15,** 693-712.

Kayser C & Logothetis NK. (2007). Do early sensory cortices integrate cross-modal information? *Brain Struct Funct* **212,** 121-132.

Kayser C, Petkov CI, Augath M & Logothetis NK. (2005). Integration of touch and sound in auditory cortex. *Neuron* **48,** 373-384.

Kayser C & Remedios R. (2012). Suppressive competition: how sounds may cheat sight. *Neuron* **73,** 627-629.

Keller GB, Bonhoeffer T & Hubener M. (2012). Sensorimotor mismatch signals in primary visual cortex of the behaving mouse. *Neuron* **74,** 809-815.

Kral A & Lomber SG. (2015). Deaf white cats. *Curr Biol* **25,** R351-353.

Land R, Baumhoff P, Tillein J, Lomber SG, Hubka P & Kral A. (2016). Cross-Modal Plasticity in Higher-Order Auditory Cortex of Congenitally Deaf Cats Does Not Limit Auditory Responsiveness to Cochlear Implants. *J Neurosci* **36,** 6175-6185.

Liang M, Mouraux A, Hu L & Iannetti GD. (2013). Primary sensory cortices contain distinguishable spatial patterns of activity for each sense. *Nat Commun* **4,** 1979.

Liao DS, Krahe TE, Prusky GT, Medina AE & Ramoa AS. (2004). Recovery of cortical binocularity and orientation selectivity after the critical period for ocular dominance plasticity. *Journal of neurophysiology* **92,** 2113-2121.

Lutcke H, Margolis DJ & Helmchen F. (2013). Steady or changing? Long-term monitoring of neuronal population activity. *Trends Neurosci* **36,** 375-384.

Macaluso E & Driver J. (2005). Multisensory spatial interactions: a window onto functional integration in the human brain. *Trends Neurosci* **28,** 264-271.

Maffei L, Fiorentini A & Bisti S. (1973). Neural correlate of perceptual adaptation to gratings. *Science* **182,** 1036-1038.

McDonald JJ, Stormer VS, Martinez A, Feng W & Hillyard SA. (2013). Salient sounds activate human visual cortex automatically. *J Neurosci* **33,** 9194-9201.

Meijer GT, Montijn JS, Pennartz CMA & Lansink CS. (2017). Audiovisual Modulation in Mouse Primary Visual Cortex Depends on Cross-Modal Stimulus Configuration and Congruency. *J Neurosci* **37,** 8783-8796.

Meredith MA, Clemo HR, Corley SB, Chabot N & Lomber SG. (2016). Cortical and thalamic connectivity of the auditory anterior ectosylvian cortex of early-deaf cats: Implications for neural mechanisms of crossmodal plasticity. *Hearing research* **333,** 25-36.

Moore BDt, Alitto HJ & Usrey WM. (2005). Orientation tuning, but not direction selectivity, is invariant to temporal frequency in primary visual cortex. *Journal of neurophysiology* **94,** 1336-1345.

Muckli L, De Martino F, Vizioli L, Petro LS, Smith FW, Ugurbil K, Goebel R & Yacoub E. (2015). Contextual Feedback to Superficial Layers of V1. *Curr Biol* **25,** 2690-2695.

Muckli L, Kohler A, Kriegeskorte N & Singer W. (2005). Primary visual cortex activity along the apparent-motion trace reflects illusory perception. *PLoS Biol* **3,** e265.

Muckli L & Petro LS. (2013). Network interactions: non-geniculate input to V1. *Curr Opin Neurobiol* **23,** 195-201.

Oliva A & Torralba A. (2007). The role of context in object recognition. *Trends Cogn Sci* **11,** 520-527.

Petro LS, Paton AT & Muckli L. (2017). Contextual modulation of primary visual cortex by auditory signals. *Philos Trans R Soc Lond B Biol Sci* **372**.

Petro LS, Smith FW, Schyns PG & Muckli L. (2013). Decoding face categories in diagnostic subregions of primary visual cortex. *Eur J Neurosci* **37,** 1130-1139.

Piche M, Chabot N, Bronchti G, Miceli D, Lepore F & Guillemot JP. (2007). Auditory responses in the visual cortex of neonatally enucleated rats. *Neuroscience* **145,** 1144-1156.

Pluta S, Naka A, Veit J, Telian G, Yao L, Hakim R, Taylor D & Adesnik H. (2015). A direct translaminar inhibitory circuit tunes cortical output. *Nat Neurosci* **18,** 1631-1640.

Poort J, Khan AG, Pachitariu M, Nemri A, Orsolic I, Krupic J, Bauza M, Sahani M, Keller GB, Mrsic-Flogel TD & Hofer SB. (2015). Learning Enhances Sensory and Multiple Non-sensory Representations in Primary Visual Cortex. *Neuron* **86,** 1478-1490.

Ramoa AS, Mower AF, Liao D & Jafri SI. (2001). Suppression of cortical NMDA receptor function prevents development of orientation selectivity in the primary visual cortex. *J Neurosci* **21,** 4299-4309.

Ringach DL, Shapley RM & Hawken MJ. (2002). Orientation selectivity in macaque V1: diversity and laminar dependence. *J Neurosci* **22,** 5639-5651.

Rockland KS & Ojima H. (2003). Multisensory convergence in calcarine visual areas in macaque monkey. *Int J Psychophysiol* **50,** 19-26.

Rockland KS & Van Hoesen GW. (1994). Direct temporal-occipital feedback connections to striate cortex (V1) in the macaque monkey. *Cereb Cortex* **4,** 300-313.

Schroeder CE & Foxe JJ. (2002). The timing and laminar profile of converging inputs to multisensory areas of the macaque neocortex. *Brain Res Cogn Brain Res* **14,** 187-198.

Schroeder CE, Smiley J, Fu KG, McGinnis T, O'Connell MN & Hackett TA. (2003). Anatomical mechanisms and functional implications of multisensory convergence in early cortical processing. *Int J Psychophysiol* **50,** 5-17.

Shuler MG & Bear MF. (2006). Reward timing in the primary visual cortex. *Science* **311,** 1606-1609.

Stevenson RA, Wallace MT & Altieri N. (2014). The interaction between stimulus factors and cognitive factors during multisensory integration of audiovisual speech. *Front Psychol* **5,** 352.

Ten Oever S, van Atteveldt N & Sack AT. (2015). Increased Stimulus Expectancy Triggers Low-frequency Phase Reset during Restricted Vigilance. *J Cogn Neurosci* **27,** 1811-1822.

van Atteveldt N, Murray MM, Thut G & Schroeder CE. (2014). Multisensory integration: flexible use of general operations. *Neuron* **81,** 1240-1253.

Vetter P, Smith FW & Muckli L. (2014). Decoding sound and imagery content in early visual cortex. *Curr Biol* **24,** 1256-1262.

Vogels R. (1999). Categorization of complex visual images by rhesus monkeys. Part 2: single-cell study. *Eur J Neurosci* **11,** 1239-1255.

Xu NL, Harnett MT, Williams SR, Huber D, O'Connor DH, Svoboda K & Magee JC. (2012). Nonlinear dendritic integration of sensory and motor input during an active sensing task. *Nature* **492,** 247-251.

Yates D. (2012). Sensory systems: sounds like competition. *Nat Rev Neurosci* **13,** 222-223.